JOURNAL OF MATERIALS SCIENCE 28 (1993) 3258–3266

Cyclic fatigue-crack propagation in a silicon carbide whisker-reinforced alumina composite: role of load ratio

R. H. DAUSKARDT, B. J. DALGLEISH, D. YAO*, R. O. RITCHIE
Center for Advanced Materials, Materials Sciences Division, Lawrence Berkeley Laboratory, and Department of Materials Science and Mineral Engineering, University of California, Berkeley, CA 94720, USA

P. F. BECHER
Metals and Ceramics Division, Oak Ridge National Laboratory, Oak Ridge, TN 37831, USA

The characteristics of subcritical crack growth by cyclic fatigue have been examined in a silicon carbide whisker-reinforced alumina composite, with specific reference to the role of load ratio (ratio of minimum to maximum applied stress intensity, $R = K_{min}/K_{max}$); results are compared with similar subcritical crack-growth data obtained under constant load conditions (static fatigue). Using compact-tension samples cycled at ambient temperatures, cyclic fatigue-crack growth has been measured over six orders of magnitude from $\sim 10^{-11}$–10^{-5} m cycle^{-1} at load ratios ranging from 0.05–0.5. Growth rates (da/dN) display an approximate Paris power-law dependence on the applied stress-intensity range (ΔK), with an exponent varying between 33 and 50. Growth-rate behaviour is found to be strongly dependent upon load ratio; the fatigue threshold, ΔK_{TH}, for example, is found to be increased by over 80% at $R = 0.05$ compared to $R = 0.5$. These results are rationalized in terms of a far greater dependency of growth rates on K_{max} ($da/dN \propto K_{max}^{30}$) compared to ΔK ($da/dN \propto \Delta K^5$), in contrast to fatigue behaviour in metallic materials where generally the reverse is true. Micromechanisms of crack advance underlying such behaviour are discussed in terms of time-dependent crack bridging involving either matrix grains or unbroken whiskers.

1. Introduction

Until recently, it had been the general perception that ceramic materials are largely insensitive to mechanical degradation under cyclic loads [1]. However, several studies, primarily over the last five years, have provided conclusive evidence that indeed ceramics do suffer cyclic fatigue under both tensile and compressive loading (see [2–4] for review). Results for both monolithic and composite ceramics have shown reduced lifetimes during stress/life (S/N) testing under cyclic, compared to quasi-static, loads, and accelerated cyclic crack-propagation rates at stress intensities less than that required for environmentally enhanced crack growth (static fatigue) during fracture-mechanics testing.

Compared to metals, cyclic fatigue-crack propagation data for a wide range of ceramic materials display a marked power-law dependency of growth rates on the applied (far-field) stress-intensity range ($\Delta K = K_{max} - K_{min}$). In simple terms, the crack-growth increment per cycle, da/dN, can be related to the applied ΔK (for "long" cracks typically in excess of a few millimetres in length) via a Paris power-law expression of the form [5]

$$da/dN = C(\Delta K)^m \quad (1)$$

where C and the exponent m are experimentally measured scaling constants dependent on the material and environmental conditions. Essentially, this behaviour is qualitatively similar to metallic materials (between typically $\sim 10^{-9}$ and $\sim 10^{-6}$ m cycle^{-1}); however, unlike metals, the exponent m can take values as high as 50 and above in ceramics [2], compared to typical values of between 2 and 4 in metals.

The very high exponents in Equation 1 reported for ceramics result from a particularly marked sensitivity of growth rates to the maximum stress-intensity factor, K_{max}, of the loading cycle (and likewise the load ratio $R = K_{min}/K_{max}$) [6, 7]. As recently shown for SiC-reinforced alumina [7], by explicitly including

* *Present address*: Department of Materials Science and Engineering, University of Illinois – Urbana-Champaign, Urbana, IL 61801, USA.

0022–2461

K_{max} in the growth-rate relationship, namely[‡]

$$da/dN = C'(K_{max})^n (\Delta K)^p \quad (2)$$

where C' is a constant equal to $C(1 - R)^n$ and $(n + p) = m$, the power-law dependencies of the growth rates on K_{max} and ΔK, as indicated by the exponents n and p, were found to be 10.2 and 4.8, respectively; this is to be compared with values of $n = 0.4$ and $p = 3$ for metal fatigue of a nickel-base superalloy [9]. The marked sensitivity of growth rates to K_{max} (or the load ratio) is similar to that seen in metals at high growth rates approaching instability, e.g. where K_{max} approaches the fracture toughness, K_{Ic}; under these conditions, mechanisms of crack growth predominantly involve static fracture modes (e.g. cleavage, microvoid coalescence, etc.) akin to mechanisms that occur under (quasi-static) monotonic loading [10]. Moreover, it is consistent with subcritical crack-growth data for both fine-grained monolithic and toughened (PSZ, whisker-reinforced alumina) ceramics under constant loading (static fatigue, stress-corrosion cracking), where crack velocities are given in terms of the applied stress intensity, K by [11–13]

$$da/dt = v = AK^s \quad (3)$$

Similar to the exponent n in the cyclic-fatigue relationship in Equation 2, values of s are very high with values up to ~ 100 [11–13].

The intent of the present study is to investigate the separate effects of K_{max} and ΔK on cyclic fatigue-crack growth behaviour in an alumina ceramic reinforced with strong, microscopic SiC whiskers. Cyclic crack-growth rates are measured over a range of load ratios and are compared with corresponding static-fatigue data obtained under constant load. Implications of the observed crack-growth dependence on both K_{max} and ΔK are discussed in the light of possible micro-mechanisms for crack advance and crack-tip shielding.

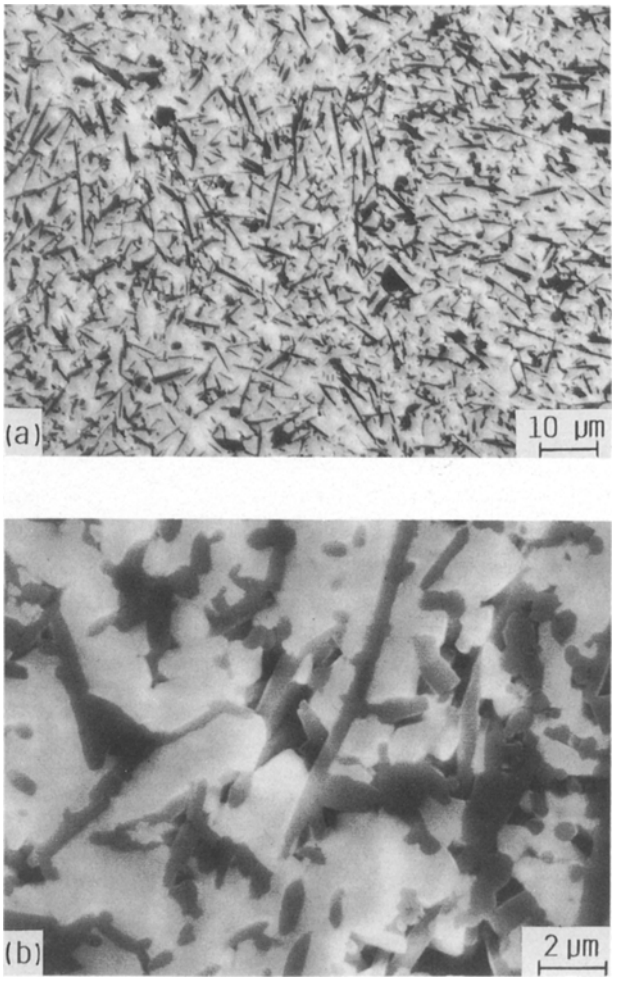

Figure 1 Scanning electron micrographs of (a) the microstructure of the SiC whisker-reinforced alumina, showing (b) local porosity centred at whisker clusters.

2. Experimental procedure

2.1. Material

Experiments were conducted on nominally fully dense samples of a SiC whisker-reinforced alumina (Al_2O_3–SiC_w), as shown in Fig. 1; whisker volume fractions of 20% and 28% were examined. The composites were prepared at Oak Ridge National Laboratory by hot pressing granulated powder consisting of a mixture of high-purity alumina powder and SiC whiskers in an inert environment. No other additives were incorporated during processing. The resulting microstructures consisted of < 10 μm sized alumina grains containing a uniform dispersion of ~ 0.8 μm diameter SiC whiskers; the whiskers had an as-received aspect ratio of up to 40, were predominantly of the α (hexagonal) form, and tended to be oriented perpendicularly to the hot-pressing direction. Some degree of local porosity was evident in the microstructure, particularly at clusters of whiskers (Fig. 1b). Further details of the processing techniques and microstructure are reported elsewhere [14, 15].

Tests specimens for both cyclic and static fatigue tests were prepared from a hot-pressed composite with the specimen oriented so that the crack plane was parallel to the axis of the hot-press die. The orientations of the long axis of the whiskers tended to lie near normal to the axis of hot pressing but were randomly oriented within the plane normal to the axis of hot pressing. Therefore, the specimen orientation used provided maximum interaction between the crack and the SiC whiskers. Two different composite compositions were tested; some of the characteristics of each are shown in Table I, and are compared with those of monolithic alumina.

2.2. Test methods

2.2.1. Cyclic fatigue

Cyclic crack-growth rates were determined under computer-controlled K-decreasing and K-increasing conditions using 3 mm thick compact-tension, C(T),

[‡] This is equivalent to the empirical model of Walker [8] commonly used to normalize load-ratio effects in metal fatigue, where an effective stress intensity, K_{eff}, is defined such that $K_{eff} = K_{max}(1 - R)^{n'}$, where n' is a material property equal to $p/(p + n)$.

TABLE I Characteristics of SiC whisker[a]-reinforced alumina composites

Sample	Whisker content (vol %)	Density ($g\,cm^{-3}$)	% theoretical density	Alumina grain size (μm)	Fracture toughness ($MPa\,m^{1/2}$)	Fracture strength (MPa)
WRA-10[b]	28	3.73	99.0	1.5	8.7 ± 0.9	–
SC-83[c]	20	3.82	99.9	9	8.7 ± 1.1	587 ± 27
Al-CR10-13	0	3.96	99.5	4	4.6 ± 0.5	250

[a] SiC whiskers F-9, Advanced Composite Materials Corp., Greer, SC, USA.
[b] Alumina powder (CR-10), Baikowski Corp., Charlotte, NC, USA.
[c] Alumina powder (Linde A), Union Carbide Corp., Indianapolis, IN, USA.

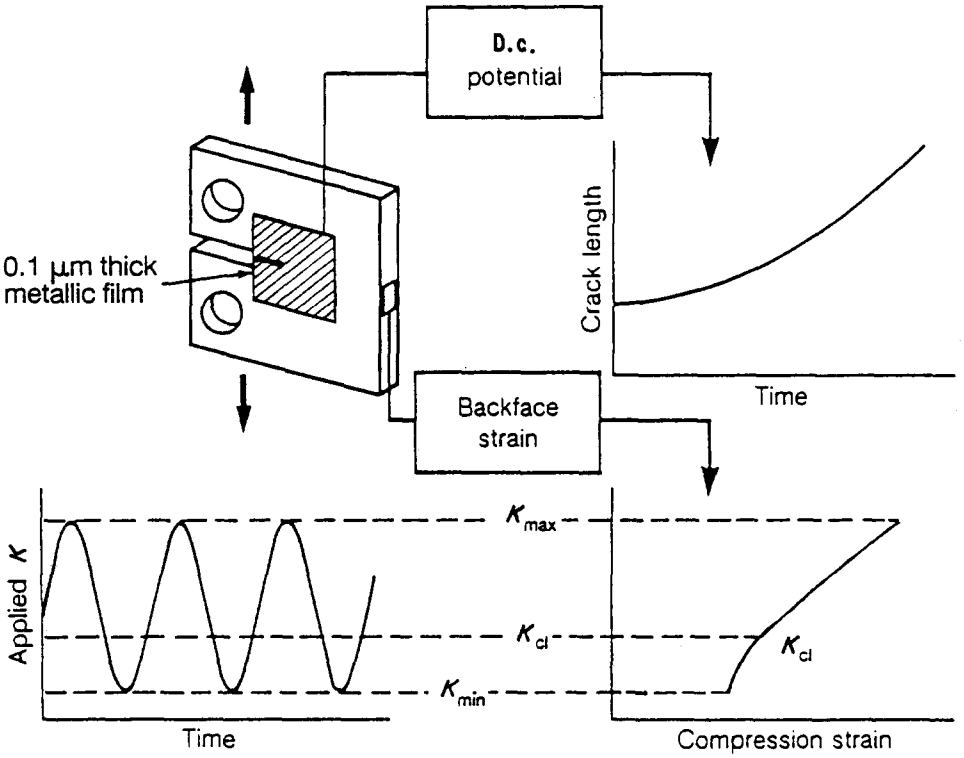

Figure 2 Experimental techniques used to measure cyclic fatigue-crack growth rates, showing compact-tension, C(T), specimen and procedures used to monitor crack length and the stress intensity, K_{cl}, at crack closure for "long" through-thickness cracks.

specimens containing long (> 3 mm) through-thickness cracks (Fig. 2). Tests were performed using high-resolution computer-controlled electro-servo-hydraulic testing machines in general accordance with the ASTM standard for measurement of fatigue-crack growth rates in metals [16], modified for ceramics using the procedures outlined by Dauskardt and Ritchie [17]. Specimens were cycled at a frequency of 25 Hz (sine wave) at selected load ratios (ratio of minimum to maximum applied loads) of 0.05, 0.1, 0.3 and 0.5; the test environment was controlled room air at $22 \pm 2\,^{\circ}C$ with $45\% \pm 5\%$ relative humidity. Growth rates were measured over the range $\sim 10^{-5}$–$10^{-11}\,m\,cycle^{-1}$ to approach a fatigue threshold, below which crack growth could not be experimentally detected. In the present experiments, thresholds are operationally defined in terms of the maximum and alternating stress intensity ($K_{max,TH}$, ΔK_{TH}) at which growth rates do not exceed $10^{-11}\,m\,cycle^{-1}$. Further experimental details are given elsewhere [17].

Crack lengths were monitored *in situ* to a resolution better than ± 2 μm, using electrical-potential measurements across ~ 0.1 μm thick NiCr foils evaporated on to the specimen surface [17, 18]. Such measurements were confirmed by periodically measuring the crack length using optical techniques. Back-face strain compliance measurements, from strain gauges bonded on to the back face of the specimen, were used to estimate the extent of fatigue crack closure [19]; the closure phenomenon results from premature contact of the crack faces on unloading due to the wedging action of, for example, fracture-surface asperities behind the crack tip [20, 21]. The degree of crack closure was assessed in terms of the closure stress intensity, K_{cl}, defined at first contact of the crack surfaces during the unloading cycle; specifically, the value of K_{cl} was calculated from the highest load where the

elastic unloading line deviated from linearity (Fig. 2) [19]. Such measurements provide a global measure of the closure stress intensity; however, they are typically insensitive to changes in closure in the immediate vicinity of the crack tip [22, 23], and, as discussed below, are difficult to interpret in material systems such as Al_2O_3–SiC where additional crack-surface contact may occur due to non-wedging phenomena such as crack bridging [24].

2.2.2. Static fatigue

Crack-growth rates under constant-loading conditions were determined using precracked ($\geqslant 4$ mm long precrack) applied-moment double cantilever-beam (AMDCB) specimens. For this specimen geometry, the applied stress intensity is independent of the crack length; thus for a given specimen size, the stress intensity can be varied simply by changing the load. In the current tests, the AMDCB samples were dead-weight loaded to raise and lower the stress intensity, and the crack-tip position was periodically monitored using an optical cathometer system which could resolve the crack tip to within $\pm$ 2 μm on the mechanically polished side surface of the test sample. The temperature and relative humidity were maintained at 22 $\pm$ 2 °C and 55% $\pm$ 5%, respectively.

2.2.3. Fracture toughness

Fracture toughness, K_{Ic}, values were obtained using the multiple indent flexture strength test method [25]. Highly polished four-point flexture bars were used with roughly five Vicker's hardness indents located on the tensile surface to provide the stress concentrator. K_{Ic} values were then estimated in the usual manner from the (maximum) load and crack length immediately prior to failure. The indentation load used was 98.07 N (10 kg).

2.2.4. Fractography

Fracture surfaces were examined using optical and scanning electron microscopy, and in profile using planar sections cut perpendicular to the crack path in the plane of loading.

3. Results and discussion

3.1. Static fatigue-growth rate behaviour

The results for the crack growth studies are shown in Fig. 3 for alumina reinforced with 20 and 28 vol % SiC whiskers and are compared to those for a dense (99.9% theoretical density) alumina ceramic with an average grain size of 4 μm (or about one-half that of the composite with 20 vol % SiC whiskers). It is clear that the onset of slow crack growth under constant loading requires a much higher applied stress intensity in the reinforced aluminas (which show essentially identical v/K behaviour). In fact, the applied stress intensity required to achieve a crack velocity of $\sim 10^{-10}$ m s^{-1} in the composites is twice that required for the unreinforced alumina. Analysis of the crack-growth response can be made based on the power-law relationship in Equation 3; values of the constant A and exponent s are listed in Table II. Regression analysis of the data represented in this form indicates a very strong dependence of the crack velocity upon the applied stress intensity for both materials, as indicated by the high s values in Table II.

TABLE II Static fatigue-crack growth parameters for Al_2O_3 and Al_2O_3–SiC_w composites

Sample	A (m s^{-1} (MPa m$^{1/2}$)$^{-s}$)	s	K_{TH} (MPa m$^{1/2}$)
Al_2O_3 (~ 4 μm grain size)	1.3×10^{-38}	55	3.2
Al_2O_3–20 vol % SiC_w (~ 9 μm grain size)	2.7×10^{-80}	81	7.1
Al_2O_3–28 vol % SiC_w (~ 2 μm grain/size)	7.2×10^{-75}	75	7.0

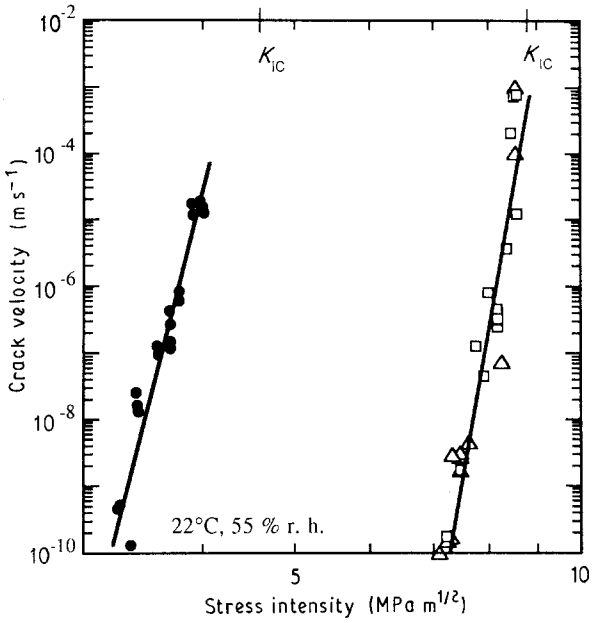

Figure 3 The onset of static fatigue-crack growth for crack velocities $\geqslant 10^{-10}$ m s^{-1} is initiated at higher applied stress intensities, K, in SiC whisker-reinforced aluminas as compared to a monolithic alumina ceramic (●). The rate of crack growth is very sensitive to changes in the applied stress intensity in each material. Composite data shown for (□) Al_2O_3–20 vol % SiC_w and (△) Al_2O_3–28 vol % SiC_w.

3.2. Cyclic fatigue-growth rate behaviour

Corresponding cyclic fatigue-crack growth rate data for load ratios of 0.05, 0.1, 0.3 and 0.5 are plotted in Fig. 4 as a function of the applied ΔK. The Al_2O_3–28 vol % SiC_w composite displays extensive cyclic fatigue-crack propagation over six orders of magnitude in growth rates; in fact, similar to metals [26], the growth-rate curves show a slightly sigmoidal shape which was reproducible under both increasing and decreasing stress-intensity conditions. Furthermore, as in metal fatigue [26], growth rates are increased, and fatigue threshold ΔK_{TH} values decreased, with increasing R; for example, ΔK_{TH} values are increased

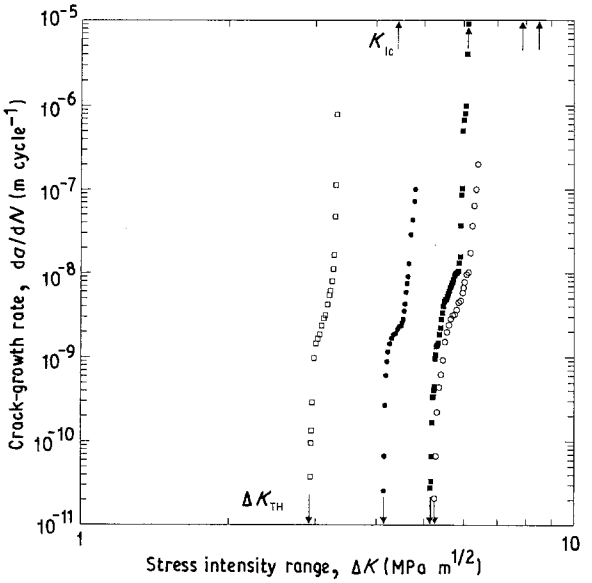

Figure 4 Variation in cyclic fatigue-crack growth rates, da/dN, in Al_2O_3–28 vol % SiC_w ceramic composite with the applied stress-intensity range ($\Delta K = K_{max} - K_{min}$), for load ratios of (○) 0.05, (■) 0.1, (●) 0.3 and (□) 0.5. Tests are performed at 25 Hz frequency in ambient temperature air (22 °C, 45% r.h.)

TABLE III Cyclic fatigue-crack growth parameters for Al_2O_3–28 vol % SiC_w composite

Load ratio R	C (m cycle^{-1} (MPa m$^{1/2}$)$^{-m}$)	m	ΔK_{TH} (MPa m$^{1/2}$)	$K_{max,TH}$ (MPa m$^{1/2}$)
0.05	5.9×10^{-34}	33	5.3	5.5
0.10	1.6×10^{-44}	48	5.2	5.7
0.30	3.5×10^{-33}	37	4.1	5.9
0.50	7.3×10^{-34}	50	2.9	5.9

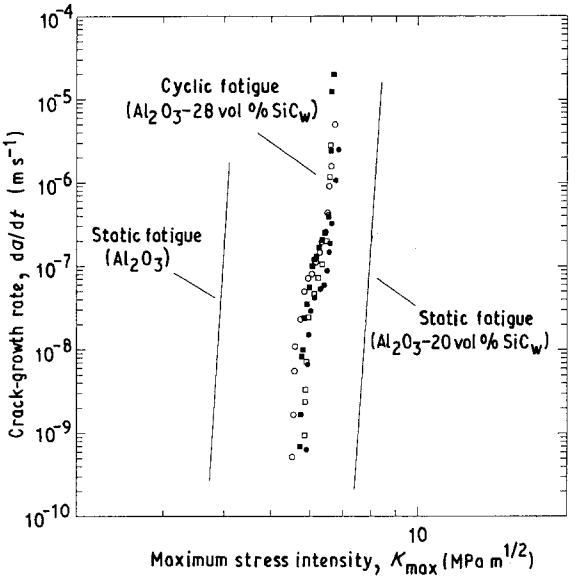

Figure 5 Comparison of cyclic fatigue-crack velocities, as a function of time, da/dt, in Al_2O_3–28 vol % SiC_w ceramic composite in ambient temperature air with the applied maximum stress intensity, K_{max} (R = 0.05–0.5), with corresponding crack-velocity data for both unreinforced Al_2O_3 and Al_2O_3–SiC_w obtained under monotonic loading (stress corrosion, static fatigue). Static fatigue data from Fig. 3.

by over 80% at $R = 0.05$ compared to $R = 0.5$. If these data are fitted to a conventional Paris law relationship (of the form of Equation 1), similar to the static-fatigue data, growth rates can be seen to display a marked power-law dependence on the applied stress intensity ranging from 33–50; moreover, values of the threshold $K_{max,TH}$ were found to be approximately 65% K_{Ic}. Both observations are similar to behaviour reported for other ceramic materials [2, 3]. Values of C, m and ΔK_{TH} at the selected load ratios are listed in Table III.

To examine the specific dependence on K_{max} and ΔK, growth-rate data were also fitted to Equation 2. In these terms, it is apparent that the steep Paris law exponents, m, are associated with a marked sensitivity of growth rates to K_{max} rather than ΔK; corresponding values of n and p are ~ 30 and 5, respectively. Resistance to cyclic fatigue-crack growth, as indicated by the value of ΔK_{TH}, is clearly sensitive to the load ratio and the entire growth-rate curve is shifted to lower values on the abscissa with increasing values of R. While such behaviour is similar to near-threshold growth rates in metallic materials where ΔK_{TH} levels are invariably decreased at higher load ratios (e.g. [26]), behaviour at higher (intermediate) growth rates (i.e. $\sim 10^{-9}$–10^{-6} m cycle^{-1}) is generally far less sensitive to the load ratio.* In fact, the effect of load ratio on growth-rate behaviour can be effectively normalized by plotting the da/dN data as a function of the maximum stress intensity, K_{max} (Fig. 5); the fatigue threshold, expressed in terms of a maximum stress intensity, $K_{max,TH}$, is essentially constant and independent of R. By representing the current results in this way, it is apparent that at a given stress intensity the velocity (with respect to time) of cyclic fatigue cracks in the Al_2O_3–SiC_w composite far exceeds that of static fatigue cracks in this material [11, 27], thereby re-affirming the essential role of the unloading cycle for the cyclic-fatigue process to occur. Crack velocities, however, are significantly slower than corresponding static-crack growth in the unreinforced Al_2O_3 matrix.

3.3. Fatigue-crack closure

Similar to behaviour widely reported for metals (e.g. [20, 21]) and in limited cases for ceramics [2, 7, 23], cyclic fatigue-crack growth behaviour in the Al_2O_3–28 vol % SiC_w composite showed evidence of crack-surface contact (i.e. "crack closure") during the fatigue loading cycle. Far-field crack-closure levels,

* Note that at very high growth rates $\gtrsim 10^{-6}$ m cycle^{-1}) approaching instability, e.g. as K_{max} approaches K_{Ic}, the marked dependence of growth rates on mean stress (or load ratio) often reappears in metallic materials as the mechanism of fatigue-crack growth involves the occurrence of "static" fracture modes, i.e. microvoid coalescence, cleavage, intergranular cracking, all mechanisms which are strongly sensitive to the tensile or hydrostatic stresses, rather than the alternating stresses *per se* [10].

defined in terms of K_{cl} and corresponding to the growth-rate data in Fig. 4 for each load ratio, are given in Fig. 6. Such closure in Al_2O_3–SiC_w appears to be caused by premature contact of rough asperities on the crack surfaces during the unloading cycle prior to minimum load. The resulting wedging effect acts to raise the effective minimum stress intensity ($K_{min} \equiv K_{cl}$), thereby lowering the effective range of stress intensity ΔK_{eff} ($K_{max} - K_{cl}$, for $K_{cl} > K_{min}$) actually experienced by the crack tip [20]. In metallic materials, replotting the growth rates for various positive load ratios in terms of ΔK_{eff}, rather than ΔK, generally will normalize the growth-rate data, as the effect of load ratio on crack velocities, particularly at near-threshold levels, is primarily associated with crack closure; higher R ratios minimize the wedging effect of closure as they involve larger crack opening displacements [19–21]. However with ceramics, this approach can be seen in Fig. 7 to have only limited success. Compared to behaviour in metallic materials (e.g. [21]), the role of crack closure in influencing cyclic crack growth in ceramic materials remains poorly understood. There is little doubt that the crack-wedging action of, for example, fracture-surface asperities will tend to diminish the crack-driving force, and as such act to retard crack-extension rates as in metals. However, whether such phenomena can be quantified in terms of a closure stress intensity remains uncertain, given that the experimental measurement of K_{cl} in terms of crack-surface contact may be clouded in many ceramics by the occurrence of other shielding mechanisms [28] such as whisker or matrix-grain bridging.

3.4. Fractography

Scanning electron microscopy observations of the static-fatigue fracture surfaces produced at crack velocities of $\sim 10^{-3}\,m\,s^{-1}$ reveal a substantial amount of transgranular fracture through the alumina grains and evidence of SiC whisker bridging and pull-out (Fig. 8). Whisker pull-out is supported by the whiskers extending above the fracture surface and by the holes where the ends of whiskers have been extracted from the matrix during fracture.

Corresponding micrographs of the fracture surfaces during overload fracture and fatigue-crack propagation at $R = 0.05$, 0.3 and 0.5 are shown in Fig. 9. Fracture surfaces are again characterized by two primary features, namely transgranular cleavage of the matrix grains (A in Fig. 9) interdispersed with the fracture and pull-out of the SiC whiskers (B in Fig. 9). The fracture morphology is only marginally changed

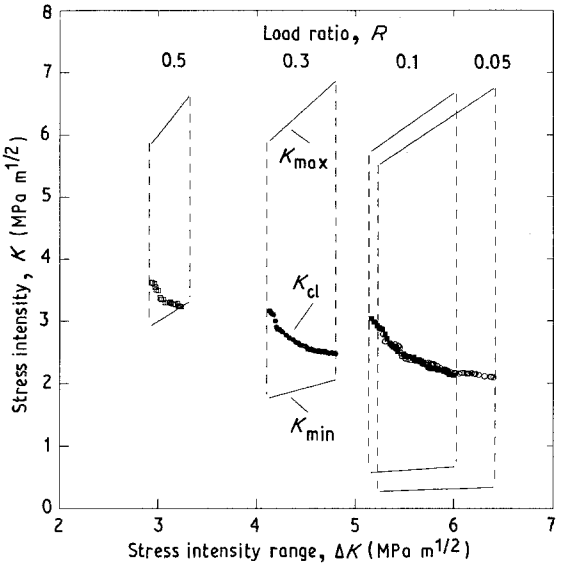

Figure 6 Experimentally measured variation in the stress intensity at closure, K_{cl}, with the applied stress-intensity range, ΔK, in Al_2O_3–28 vol% SiC_w ceramic composite during cyclic fatigue in ambient temperature air for load ratios of 0.05, 0.1, 0.3 and 0.5. Applied values of K_{max} and K_{min} are shown for comparison. 25 Hz, 22 °C, 45% r.h.

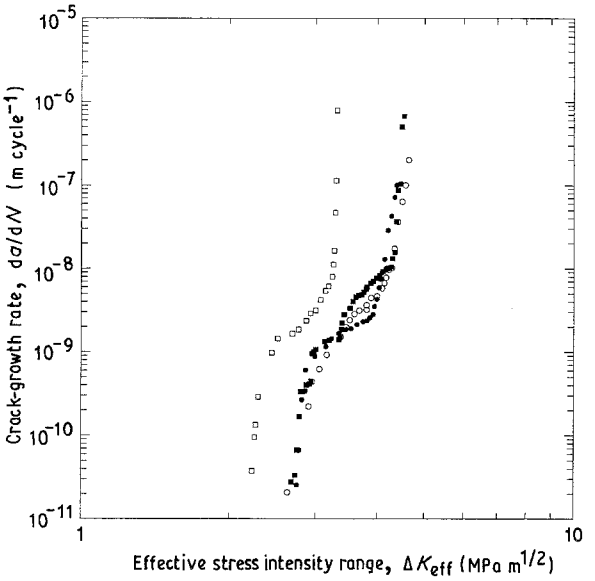

Figure 7 Variation in cyclic fatigue-crack growth rates, da/dN, in Al_2O_3–28 vol% SiC_w ceramic composite at ambient temperature with the effective stress-intensity range ($\Delta K_{eff} = K_{max} - K_{cl}$), for load ratios of (○) 0.05, (■) 0.1, (●) 0.3 and (□) 0.5. 25 Hz, 22 °C, 45% r.h.

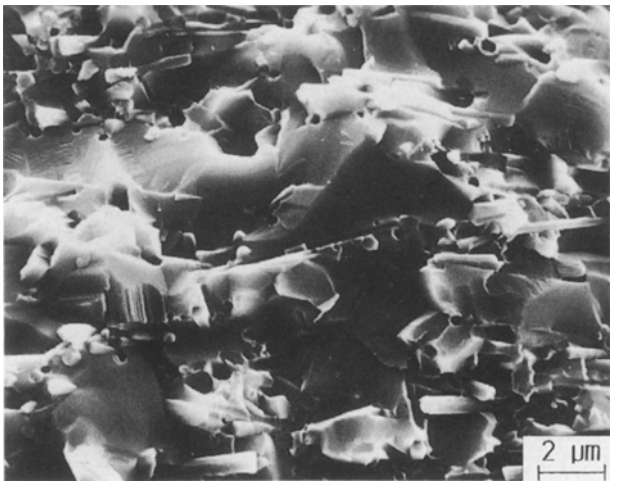

Figure 8 Extensive transgranular fracture of the alumina grains and pull-out of the SiC whiskers are observed on fracture surfaces produced at high crack velocities in the larger grained alumina reinforced with 20 vol% SiC whiskers, during static fatigue-crack growth.

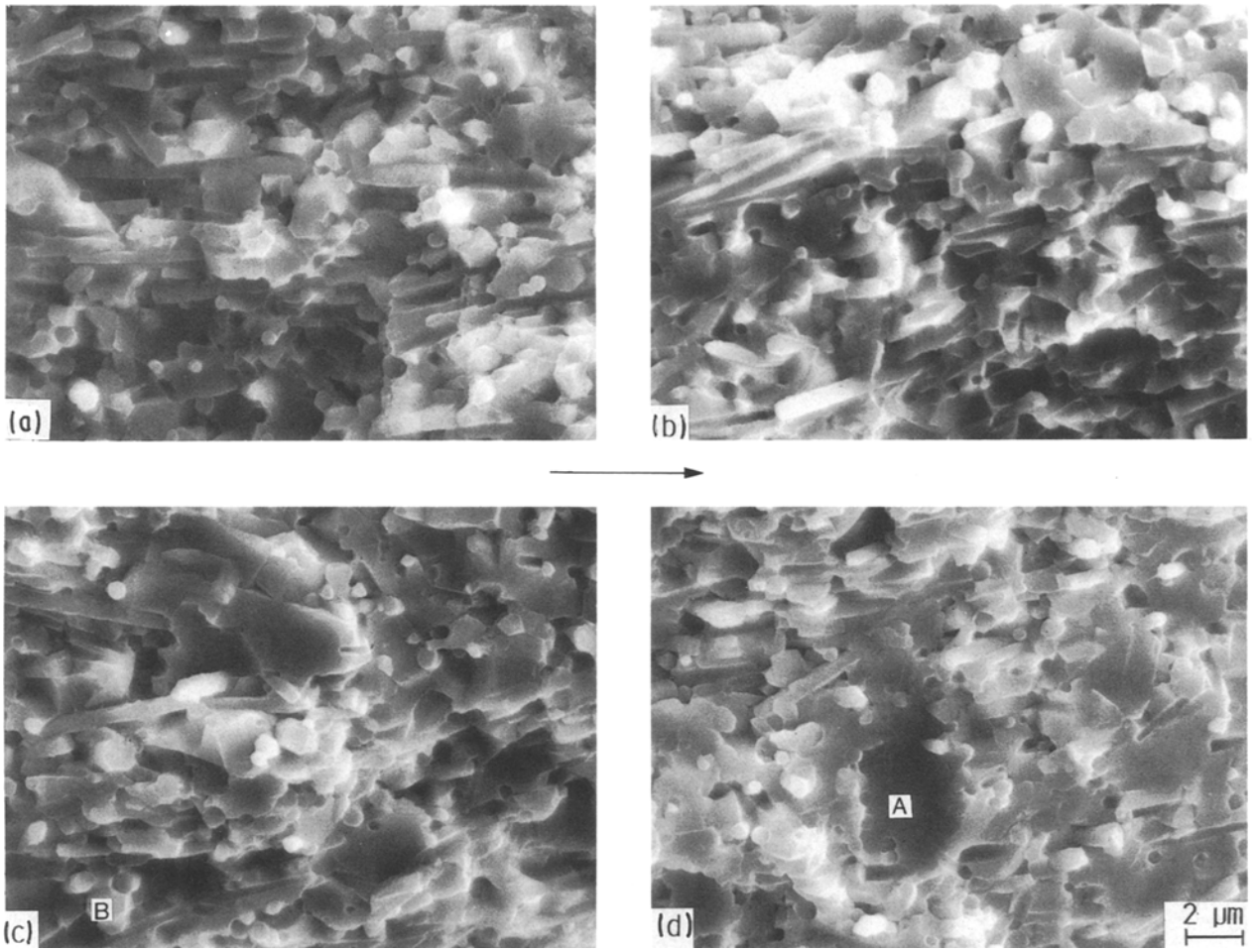

Figure 9 Scanning electron micrographs showing the fractography of cyclic fatigue-crack propagation in Al_2O_3–28 vol % SiC_w ceramic composite at load ratios of (a) 0.05, (b) 0.3, and (c) 0.5, and (d) overload fracture. Regions of transgranular cleavage of matrix grains and SiC whisker fracture/pull-out are indicated by A and B, respectively. Arrow indicates the general direction of crack growth for all micrographs.

at the differing load ratios and is, in fact, very similar for failure under either monotonic or cyclic loading. However, there is evidence of somewhat more whisker pull-out in cyclic fatigue and more matrix-grain cleavage under monotonic loads (c.f. Fig. 9d with 9a). Moreover, for the cyclic fatigue surfaces, the proportion of transgranular cleavage facets does appear to increase slightly with increasing load ratio.

On examination of the cyclic fatigue fractures by metallographic sectioning (Fig. 10), it is apparent that the crack path frequently tends to seek out regions of local porosity (C in Fig. 10). The interaction of the fatigue crack with the SiC whiskers in general involves either whisker fracture (D in Fig. 10) or debonding along the whisker/matrix interface (E in Fig. 10), with little change in crack-path direction; however, there are examples of significant crack deflection where the crack encounters the larger whiskers (F in Fig. 10). *In situ* observations of crack propagation reveal the occurrence of matrix-grain bridging behind the crack tip; however, no evidence of crack bridging by intact whiskers could be detected.

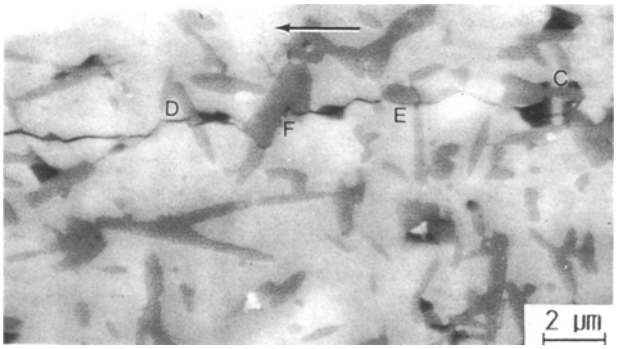

Figure 10 Scanning electron micrograph of the profile of a cyclic fatigue crack in Al_2O_3–28 vol % SiC_w ceramic composite at a load ratio of 0.05. Note that the crack path follows regions of local porosity (C), and results in both whisker fracture (D) and failure along whisker/matrix interfaces (E) with little evidence of crack deflection, except at large SiC whiskers (F). Arrow indicates the general direction of crack growth.

3.5. Mechanisms of crack growth

Previous studies [14, 15, 28, 29] on monotonic crack propagation and fracture-toughness behaviour have shown that the principal contributions to crack-growth resistance in the present Al_2O_3–SiC_w composite system result from crack bridging by partially bonded SiC whiskers, subsequent pull-out of these whiskers, bridging and pull-out of matrix grains, and to a small extent from crack deflection. The increases in toughness induced by the bridging processes derive

from tractions imposed on the crack surfaces by the whiskers and grains, which vary with increases in the crack opening displacement behind the crack tip.

For frictional bridging by partially debonded whiskers, large radial stresses are imposed on the debonding interfaces by the thermal expansion mismatch between SiC and Al_2O_3. Thus, although the whiskers are relatively strong ($\sim$ 8–16 GPa) [30], the bridging stresses supported by these whiskers increase very rapidly as the crack opens such that whisker fracture ensues a short distance behind the crack tip. This implies that the zone of unbroken whiskers in the wake of the crack tip (the frictional whisker-bridging zone) is quite small; experimental measurements [29] suggest dimensions of the order of 10 μm behind the crack tip. However, bridging via whisker pull-out, where whisker rupture occurs well away from the crack plane, can be active at distances several hundreds of micrometers behind the crack tip [31]; this process requires considerable energy as the mismatch in thermal expansion imposes significant radial compressive stresses on the sliding interface.

Compared to frictional bridging via whiskers, crack bridging by interlocking matrix grains results in much lower bridging stresses; however, the crack-opening displacement required to pull out a matrix grain is much larger. Correspondingly, bridging zones for this mechanism have been estimated to extend for several hundred micrometres behind the crack tip [32, 33], and are generally considered to provide a significant toughening contribution. When the matrix grain size is very fine (e.g. less than 2 μm), however, matrix grain bridging appears to be far less significant for toughness than whisker bridging and pull-out [15].

These multiple bridging mechanisms have been shown to combine to give an increased fracture resistance equal to the sum of the toughening contribution from each mechanism [15]. However, under cyclic loading, their contribution to crack-growth resistance may be progressively diminished due to a decay of the frictional sliding resistance of the matrix/bridge interfaces. While detailed models of the micromechanics of such time-dependent bridging phenomena are at present not well developed, some preliminary observations [2, 7, 34–38] seem to suggest that wear processes during repeated sliding under the action of the cyclic loads may significantly reduce the bridging capacity of the bridging zone.

In general, such wear degradation may be expected to scale with the matrix/bridge sliding distance, resulting in a more pronounced decrease in the bridging zone capacity with increased cyclic crack opening displacements, that is, with decreasing load ratio, R. As discussed earlier, however, growth rates in this ceramic composite are particularly sensitive to the tensile stress state ahead of the crack tip and hence the maximum stress intensity, K_{max}, and far less sensitive to the range of stress intensity, ΔK, as suggested by the above time-dependent bridging mechanism. Growth rates must therefore be interpreted in terms of contributions from both fracture processes at or ahead of the crack tip, which are particularly sensitive to K_{max} ($da/dN \propto K_{max}^{30}$) and relatively insensitive to ΔK, and wear degradation of the bridging zone capacity behind the crack tip, which is dependent on ΔK ($da/dN \propto \Delta K^5$). Plots of crack-growth rate data, presented in terms of K_{max} should, therefore, be expected to be shifted slightly to lower stress intensities with decreasing stress-intensity range or increasing load ratio. While such behaviour is only marginally apparent within the overall scatter of growth-rate data reported in the present study (Fig. 4), with improvements in the accuracy of data and more homogeneous materials, the effect is expected to be more apparent.

4. Conclusions

Based on a study of the role of load ratio in influencing cyclic fatigue-crack propagation in SiC whisker-reinforced alumina-matrix composites (Al_2O_3–SiC_w), the following conclusions can be drawn.

1. Rates of cyclic fatigue-crack growth (da/dN) over the range $\sim 10^{-11}$–10^{-5} m cycle^{-1} are found to be power-law dependent upon the applied stress-intensity range ΔK, with an exponent varying between 33 and 50. Similar high dependencies on the applied stress intensity are observed for static fatigue-crack growth under constant loading conditions.

2. Crack-growth rates and the value of the fatigue threshold ΔK_{TH} are found to be strongly influenced by the load ratio (over the range $R = 0.05$–0.5); specifically, values of ΔK_{TH} are increased by over 80% at $R = 0.05$ compared to $R = 0.5$. Values of $K_{max,TH}$ are approximately 65% K_{Ic} for all load ratios.

3. The effect of load ratio on crack-growth behaviour is rationalized in terms of a far greater dependency of growth rates on the maximum, rather than the alternating, stress intensity; i.e. $da/dN \propto K_{max}^{30}\Delta K^5$. Unlike metallic materials, considerations on the role of crack closure in influencing the effective crack-driving force do not provide a complete normalization of the load-ratio data.

4. The driving force for cyclic fatigue-crack growth in Al_2O_3–SiC_w is reasoned to be strongly affected by micro-mechanisms of crack bridging from interlocking matrix grains and intact whiskers and subsequent pull-out. Specifically, compared to crack growth under monotonic loading, the near-tip stress intensity in cyclic fatigue is enhanced by a diminished effect of such bridging due to a time-dependent decay in the strength of the matrix/bridge interfaces.

Acknowledgements

This work was supported by the Director, Office of Energy Research, Office of Basic Energy Sciences, Materials Sciences Division of the US Department of Energy, through Contract DE-AC03-76SF00098 at Berkeley and Contract DE-AC05-84OR21400 with Martin Marietta Energy Systems, Inc., at Oak Ridge.

References

1. A. G. EVANS, *Int. J. Fract.* **16** (1980) 485.
2. R. O. RITCHIE and R. H. DAUSKARDT, *J. Ceram. Soc. Jpn* **99** (1991) 1047.

3. J. W. HOLMES, in "Flight-Vehicle Materials, Structures and Dynamics Technologies – Assessment and Future Directions", edited by A. K. Noor and F. L. Venneri Vol. 3 (American Society for Mechanical Engineers, New York, 1992) p. 193.
4. S. SURESH, *Int. J. Fract.* **42** (1990) 41.
5. P. C. PARIS and F. ERDOGAN, *J. Bas. Engng Trans. ASME* **85** (1963) 528.
6. S.-Y. LIU and I.-W. CHEN, *J. Amer. Ceram. Soc.* **74** (1991) 1197.
7. R. H. DAUSKARDT, M. R. JAMES, J. R. PORTER and R. O. RITCHIE, *ibid.* **75** (1992) 759.
8. K. WALKER, ASTM STP 462 (American Society for Testing and Materials, Philadelphia, PA, 1970) p. 1.
9. R. H. VAN STONE, *Mater. Sci. Engng* **A103** (1988) 49.
10. R. O. RITCHIE and J. F. KNOTT, *Acta Metall.* **21** (1973) 639.
11. P. F. BECHER, *J. Amer. Ceram. Soc.* **66** (1983) 485.
12. P. F. BECHER and M. K. FERBER, *Acta Metall.* **33** (1985) 1217.
13. P. F. BECHER, *J. Mater. Sci.* **21** (1986) 297.
14. P. F. BECHER, C. H. HSEUH, P. ANGELINI and T. N. TIEGS, *J. Amer. Ceram. Soc.* **71** (1988) 1050.
15. P. F. BECHER, E. R. FULLER Jr and P. ANGELINI, *ibid.* **74** (1991) 2131.
16. ASTM Standard E647-88a, "Standard Test Method for Measurement of Fatigue Crack Growth Rates", in "1989 ASTM Annual Book of Standards", Vol. 3.01 (American Society for Testing and Materials, Philadelphia, PA, 1989) p. 646.
17. R. H. DAUSKARDT and R. O. RITCHIE, *Closed Loop* **17** (1989) 7.
18. P. K. LIAW, H. R. HARTMANN and W. A. LODGSON, *J. Test. Eval.* **11** (1983) 202.
19. R. O. RITCHIE and W. YU, in "Small Fatigue Cracks", edited by R. O. Ritchie and J. Lankford (TMS-AIME, Warrendale, PA, 1986) p. 167.
20. W. ELBER, in "Damage Tolerance in Aircraft Structures", ASTM STP 486 (American Society for Testing and Materials, Philadelphia, PA, 1971) p. 230.
21. S. SURESH and R. O. RITCHIE, in "Fatigue Crack Growth Threshold Concepts", edited by D. L. Davidson and S. Suresh (TMS-AIME, Warrendale, PA, 1984) p. 227.
22. C. M. WARD-CLOSE and R. O. RITCHIE, in "Mechanics of Fatigue Crack Closure", ASTM STP 982 (American Society for Testing and Materials, Philadelphia, PA, 1988) p. 93.
23. R. H. DAUSKARDT, D. B. MARSHALL and R. O. RITCHIE, *J. Amer. Ceram. Soc.* **73** (1990) 893.
24. A. G. EVANS, in "Fracture Mechanics: Perspectives and Directions (Twentieth Symposium)", ASTM STP 1020 (American Society for Testing and Materials, Philadelphia, PA, 1989) p. 267.
25. R. COOK and B. R. LAWN, *J. Amer. Ceram. Soc.* **66** (1983) C200.
26. R. O. RITCHIE, *Int. Met. Rev.* **20** (1979) 205.
27. P. F. BECHER, T. N. TIEGS, J. C. OGLE and W. A. WARWICK, in "Fracture Mechanics of Ceramics", Vol. 7, edited by R. C. Bradt, A. G. Evans, D. P. H. Hasselman and F. F. Lange (Plenum, New York, 1986) p. 61.
28. P. F. BECHER, *J. Amer. Ceram. Soc.* **74** (1991) 255.
29. P. ANGELINI, W. MADER and P. F. BECHER, in "Advanced Structural Ceramics, MRS Proceedings", Vol. 78, edited by P. F. Becher, M. V. Swain and S. Somiya (Materials Research Society, Pittsburgh, PA, 1987), p. 241.
30. J. J. PETROVIC and R. C. HOOVER, *J. Mater. Sci.* **22** (1987) 517.
31. J. RÖDEL, E. R. FULLER Jr and B. R. LAWN, *J. Amer. Ceram. Soc.* **74** (1991) 3154.
32. P. L. SWANSON, C. J. FAIRBANKS, B. R. LAWN, Y. W. MAI and B. J. HOCKEY, *J. Am. Ceram. Soc.* **70** (1987) 279.
33. G. VEKINIS, M. F. ASHBY and P. W. R. BEAUMONT, *Acta Metall. Mater.* **38** (1990) 115.
34. S. LATHABAI, J. RÖDEL and B. R. LAWN, *J. Amer. Ceram. Soc.* **74** (1991) 1340.
35. R. O. RITCHIE, R. H. DAUSKARDT, W. YU and A. M. BRENDZEL, *J. Biomed. Mater. Res.* **24** (1990) 189.
36. F. GUIU, M. J. REECE and D. A. J. VAUGHAN, *J. Mater. Sci.* **26** (1991) 3275.
37. H. KISHIMOTO, A. UENO and H. KAWAMOTO, in "Fatigue of Advanced Materials", edited by R. O. Ritchie, R. H. Dauskardt and B. N. Cox (Materials and Component Engineering Publications, Birmingham, UK, 1991) p. 255.
38. X.-Z. HU and Y.-W. MAI, *J. Amer. Ceram. Soc.* **75** (1992) 848.

Received 6 April
and accepted 5 November 1992